# Application of acoustic imaging techniques on snowmobile pass-by noise

Thomas Padois, Alain Berry

▶ **To cite this version:**

Thomas Padois, Alain Berry. Application of acoustic imaging techniques on snowmobile pass-by noise. Journal of the Acoustical Society of America, 2017, 141, pp.EL134. 10.1121/1.4976138 . hal-01478222

**HAL Id: hal-01478222**
**https://hal.science/hal-01478222**

Submitted on 28 Feb 2017

**HAL** is a multi-disciplinary open access archive for the deposit and dissemination of scientific research documents, whether they are published or not. The documents may come from teaching and research institutions in France or abroad, or from public or private research centers.

L'archive ouverte pluridisciplinaire **HAL**, est destinée au dépôt et à la diffusion de documents scientifiques de niveau recherche, publiés ou non, émanant des établissements d'enseignement et de recherche français ou étrangers, des laboratoires publics ou privés.

Distributed under a Creative Commons Attribution 4.0 International License

# Application of acoustic imaging techniques on snowmobile pass-by noise

**Thomas Padois and Alain Berry**
*Groupe d'Acoustique de l'Université de Sherbrooke (GAUS)—Department of Mechanical Engineering, Université de Sherbrooke, 2500 boulevard de l'université, Sherbrooke (Qc) J1K 2R1 Canada*
*thomas.padois@usherbrooke.ca, alain.berry@usherbrooke.ca*

**Abstract:** Snowmobile manufacturers invest important efforts to reduce the noise emission of their products. The noise sources of snowmobiles are multiple and closely spaced, leading to difficult source separation in practice. In this study, source imaging results for snowmobile pass-by noise are discussed. The experiments involve a 193-microphone Underbrink array, with synchronization of acoustic with video data provided by a high-speed camera. Both conventional beamforming and Clean-SC deconvolution are implemented to provide noise source maps of the snowmobile. The results clearly reveal noise emission from the engine, exhaust, and track depending on the frequency range considered.

## 1. Introduction

The snowmobile was invented at the beginning of the 20th century for military use. It became a recreational vehicle in the 1960s when J. A. Bombardier, a Quebec inventor, conceived a revolutionary track suitable for many types of snow. Nowadays in Quebec, 800 000 people use a snowmobile during the winter.[1] The snowmobile trail network in Quebec totals more kilometers than the road network and the number of snowmobiles has increased by 1.5% a year since 2001.[1] This democratization of the snowmobile has forced manufacturers to reduce the noise level of their products.

The noise emitted by snowmobiles is a complex combination of airborne and structure borne radiation from the engine, exhaust, transmission, and track. According to SAE standard J192,[2] snowmobile pass-by noise is measured using a single static microphone at a distance of 15.2 m from the snowmobile. This results in an acoustic index, called $L_{A\max}$, that corresponds to the overall sound pressure level in dB(A).[3,4] Since the 1970s, this $L_{A\max}$ index has decreased by 15 dB(A) due to the development of new technologies.[1] However microphone array techniques have never been applied to snowmobile pass-by noise to the authors knowledge. The main advantage of microphone array techniques as compared to the current SAE-J192 standard is the ability to detect the positions and the strengths of noise sources in relation to the frequency. Given the relatively small separation of noise sources on a snowmobile, the microphone array has to be located at a short distance from the pass-by vehicle. This also alleviates the effect of environmental conditions (wind, temperature, ground absorption) that impact microphone measurements.[2]

The conventional microphone array processing, beamforming, has been widely used in the last two decades.[5,6] Barsikow *et al.*[7] have carried out beamforming measurements on high speed trains with a linear microphone array to detect the wheel-rail noise. In the case of rapidly moving sources, such as train or aircraft, one challenge is to take into account the Doppler effect in order to compensate for both frequency shift and apparent source level variation due to source motion.[8] Recent improvements involve the use of two cameras associated to a cross-shape microphone array to accurately follow the moving source.[9] In this work, an Underbrink 193-microphone array associated to a camera is used to detect the snowmobile noise sources. Classical beamforming and deconvolution techniques are tested to achieve proper spatial resolution of the sources.

Section 2 introduces the sound source localization techniques used. The experimental setup is presented in Sec. 3. Finally, sound source localization results on a Ski-Doo snowmobile are reported in Sec. 4.

## 2. Source localization methods

### 2.1 Beamforming

The most common technique to process phased array data is beamforming. This technique has been widely studied in the last two decades for aeroacoustic problems.[10–12] For sake of conciseness, beamforming principles are only briefly recalled. The microphone time signals are used to compute the microphone Cross Spectral Matrix (CSM) denoted $\mathbf{C}(\omega)$, which has dimensions $[M \times M]$ with $M$ the number of microphones and $\omega$ the angular frequency. The aim of beamforming is to delay and sum all microphone signals in relation to virtual source positions defined to be a series of $S$ scan points. The output beamforming $\mathbf{Q_{BF}}$ is given by

$$\mathbf{Q_{BF}}(\omega) = \mathbf{W}(\omega)^H \mathbf{C}(\omega)\mathbf{W}(\omega), \tag{1}$$

where $\mathbf{W}(\omega)$ is the normalized steering vector and $(\cdot)^H$ the Hermitian transpose. The size of $\mathbf{W}(\omega)$ is $[M \times S]$ and it is given by

$$\mathbf{W}(\omega) = \frac{\mathbf{G}(\omega)}{\sum_M |\mathbf{G}(\omega)|^2}, \tag{2}$$

where $\mathbf{G}(\omega)$ $[M \times S]$ is the matrix of free-field Green functions between individual scan points and microphone positions, defined by $\mathbf{G}(\mathbf{x}_m, \mathbf{x}_s) = (1/4\pi\|\mathbf{x}_m - \mathbf{x}_s\|)\exp(-j\mathbf{k}\|\mathbf{x}_m - \mathbf{x}_s\|)$, $\mathbf{x}_s$, $\mathbf{x}_m$ and $\mathbf{k}$ are, respectively, the scan point and microphone positions and the acoustic wave number. Basically, a beamforming noise source map exhibits a large main lobe at low frequency with side lobes due to the finite aperture and spatial sampling of the microphone array. To improve the resolution of beamforming noise source maps many deconvolution techniques have been developed such as Clean-SC,[13] DAMAS,[14] or Refs. 15 and 16.

### 2.2 Clean-SC

Clean-SC is one of the most commonly employed deconvolution techniques in aeroacoustics due to its efficiency and low computation time. Clean-SC (Ref. 13) removes side lobes and spots spatially coherent with the main lobe obtained by beamforming. Moreover the size of the main lobe is clearly reduced as compared to beamforming. The iterative process of Clean-SC is briefly introduced here, for more information the reader can refer to Ref. 13. In the initial step, the delay-and-sum beamforming noise source map is computed, then the peak value is found. A new CSM due to the source distribution coherent with the peak value is constructed. The new CSM is subtracted from the initial one and the process is repeated iteratively. At the end, the peak values are replaced by monopolar point sources and added to the residual noise source map. In this paper the noise source maps given by Clean-SC and beamforming are compared.

## 3. Experimental setup

An experiment has been carried out at a snowmobile test trail in winter. The trail consists of a 3 km open straight line with a low background noise. The microphone array was placed vertically at 2.8 m from the center of the trail and consisted of 193 microphones placed along 16 spiral arms with 12 microphones per arm plus one at the center [see Fig. 1(a)]. The microphones were installed on a grid which was fixed to an aluminum frame. The size of the microphone array was 3.15 m and 2.2 m in the horizontal and vertical directions. The microphones were Bruel&Kjaer (Denmark) array microphones model No. 4957 and the signals were acquired with 17 LAN-XI synchronized modules. The acoustic signals were sampled at 32 768 Hz. The acquisition started when the snowmobile was at 10 m from the microphone array and concluded at 10 m in the opposite direction. The snowmobile pass-by was recorded by a high speed video camera (Casio (Japan) Exilim FC-100, 210 frames per second) located opposite to the microphone array at 8 m. Therefore the camera does not see the same snowmobile side as the microphone array. The video and the acoustic signals were synchronized with two deflectors located 4 m before and after the center of the microphone array. When the snowmobile passed in front of the deflectors, rising edges were recorded by the acquisition modules and a red light was switched on. The video of the pass-by was transformed into frames and the first and last frames correspond to instants where the red lights are switched on. In order to determine the snowmobile position on the frames, lines separated by 1 m were painted on the ground. The acoustic signal before and after the rising-edges were eliminated and the useful portion was divided into $L$ blocks of $N$ samples. The CSM was computed for each of the $L$-blocks and associated to a frame. Finally the CSM was used to perform beamforming and

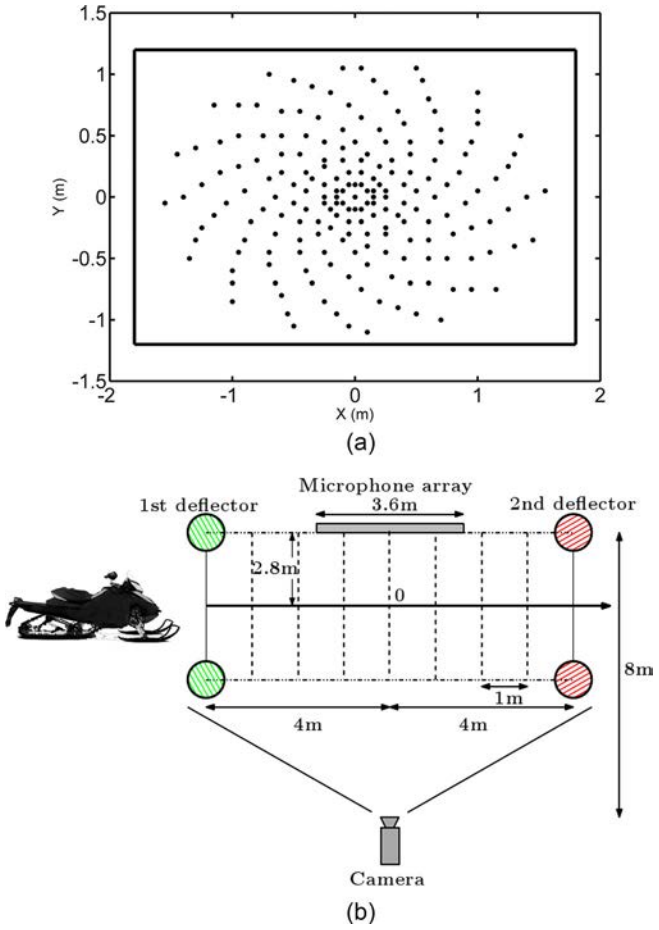


Fig. 1. Schematic of (a) the microphone array geometry and (b) the experimental setup.

Clean-SC calculations. For the snowmobile speeds considered, the Doppler Effect is low and was therefore not considered. For the scan zone considered, the influence of ground reflection is small; no correction for ground reflection was therefore implemented in the results. On the noise source map figures, only normalized sound levels are shown because of confidentiality issues with the industrial partner.

## 4. Sound source localization techniques applied to snowmobile pass-by

### *4.1 Snowmobile pass-by noise: Case of a controlled acoustic source*

Before performing the sound source localization on the snowmobile pass-by, the experimental process was tested with a controlled acoustic source on a 900 ACE Ski-Doo in order to validate the synchronization of the video and acoustic data. The controlled acoustic source was a buzzer held by the pilot's hand close to the handlebar and oriented toward the microphone array; this buzzer generates sound at 2800 Hz. Therefore, the source position and the frequency content were well known. This buzzer has been chosen because the tone clearly emerges in the power spectral density of microphone signals. The snowmobile was driven by a professional pilot who was able to keep a constant speed of 20 km/h along the trail. The acoustic and video data were processed as explained in Sec. 3. The acoustic signal contains 58 937 samples divided into 20 time-blocks, corresponding to successive positions for which source imaging algorithms were implemented. Therefore, for each time block of 2946 samples (frequency resolution of $\Delta f = 11$ Hz), the various imaging methods were implemented in the frequency domain following a Fourier transform of the corresponding time block without average or overlap. The CSM of microphone signals was computed for each block and associated to a video frame. The scan zone where the sources were searched was a square with 4 m side sampled with 101 points in each direction, giving a minimum source separation of 4 cm. The scan zone is fixed in the snowmobile reference frame. Figure 2 shows the noise source maps when the snowmobile is in front of the microphone array. In each case, the source level is normalized by the peak value. The dynamic range of noise source map is 15 dB and one color corresponds to 1 dB. The

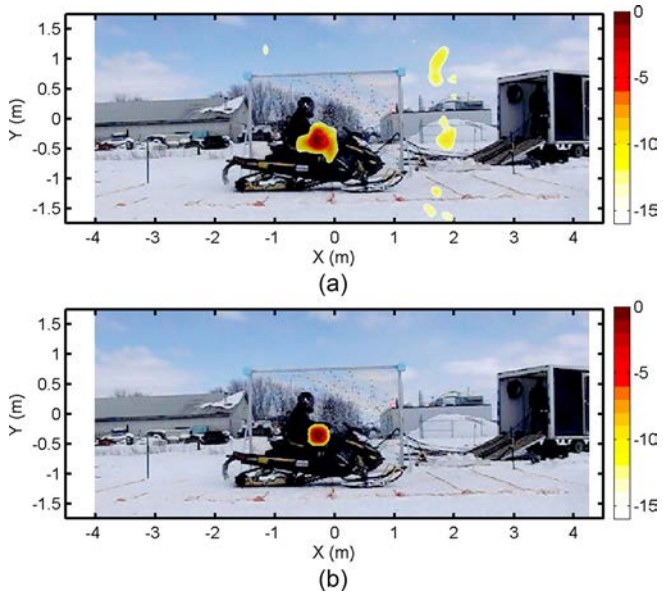


Fig. 2. Noise source maps for a snowmobile pass-by with a controlled acoustic source held by the pilot. (a) Beamforming technique and (b) Clean-SC technique. The color bar is in dB and one color level represents 1 dB.

beamforming map reveals a main spot close to the pilot's hand. Therefore, the controlled acoustic source is well detected. Spurious lobes also visible are probably due to the point spread function of the array. In order to remove these spurious lobes, deconvolution techniques such as Clean-SC can be used. The noise source map obtained with Clean-SC is shown in Fig. 2(b). With Clean-SC, the spurious lobes are removed and the main lobe is narrower and exactly at the buzzer position. Therefore, this first experiment has shown that beamforming and Clean-SC can detect the position of a controlled acoustic source on the snowmobile. Moreover, Clean-SC clearly improves the source map and allows an accurate detection of the source position. In Sec. 4.2, the sound source localization techniques are applied to snowmobile pass-by noise.

### *4.2 Snowmobile pass-by: Effect of engine hood*

Engine hoods are commonly used to protect the engine from the external environment and reduce engine noise emissions. On the tested snowmobile (MXZ Ski-Doo), the engine hood is a panel with attached acoustic treatment, located on the right-hand-side

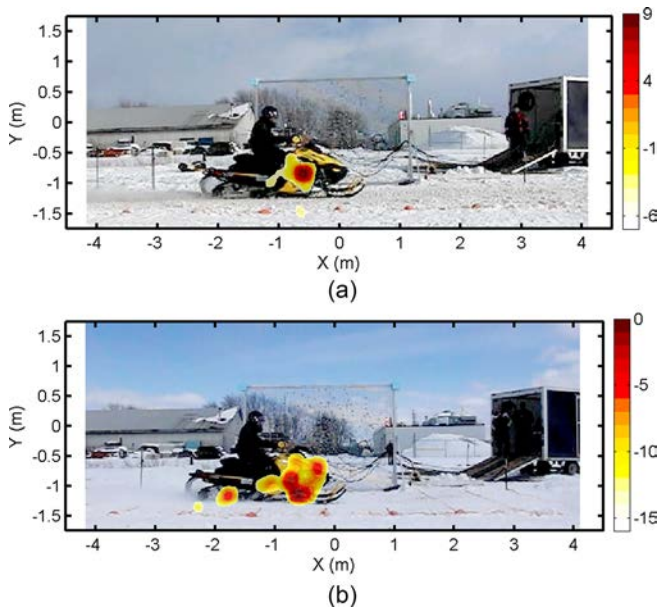


Fig. 3. (Color online) Clean-SC noise source maps in the frequency range [1000–1500] Hz for a snowmobile pass-by at 70 km/h, (a) without engine hood and (b) with engine hood. The color bar is in dB and one color level represents 1 dB.

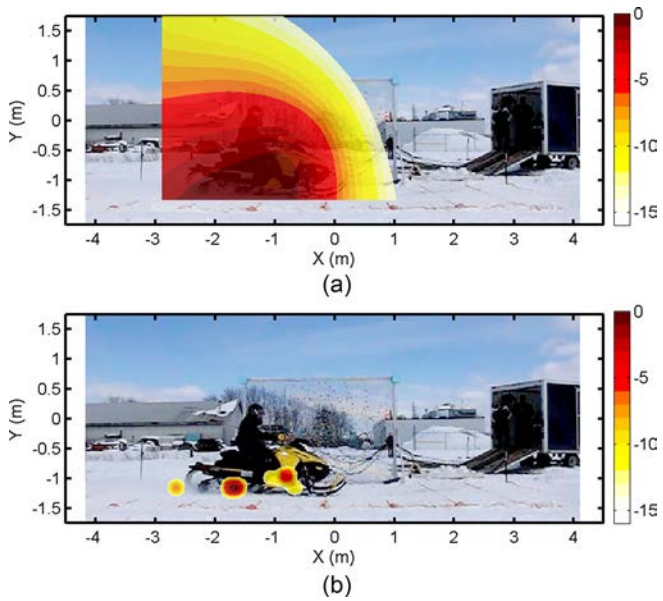


Fig. 4. Noise source maps in the frequency range [200–800] Hz for a snowmobile pass-by at 70 km/h, (a) beamforming technique and (b) Clean-SC technique. The color bar is in dB and one color level rep-resents 1 dB.

of the vehicle [see Fig. 3(b)]. In order to estimate the acoustic insertion loss provided by the engine hood, pass-by tests have been carried out with and without the engine hood. The acoustic imaging algorithms have been implemented in the frequency range [1000–1500] Hz for which previous tests showed that engine noise is dominant. In this case, the noise source maps were generated for each frequency sample and summed over the investigated frequency range. The snowmobile speed was set to 70 km/h (maximum speed in Quebec). Only Clean-SC results are shown due to higher performance. The noise source maps have been normalized by the peak value in the case where the engine hood was present. The noise source map without engine hood is presented in Fig. 3(a) and exhibits a single spot at the engine location. This demonstrates the effectiveness of the engine noise source localization. As the engine tone clearly emerges in the power spectral density of sound pressure signals, no other sources are visible. When the engine hood is present [Fig. 3(b)], the peak source level is approximately 9 dB smaller than in the situation where the hood has been removed. Moreover, the main spot is now moved below the engine location and is more extended, showing areas which radiate engine noise. Also two other spots correspond to a part of the track and the exhaust which contribute to the total sound radiation in the frequency range investigated.

### *4.3 Snowmobile pass-by noise: Broadband noise*

In this section the aim was to estimate the ability of the source imaging algorithms to detect low-frequency broadband noise, for which the beamforming resolution was known to be poor. The snowmobile speed was set to 70 km/h and the data process was the same as in Sec. 4.1. Both beamforming and Clean-SC were processed in the frequency range [200–800] Hz. The beamforming noise source map [Fig. 4(a)] exhibits a main lobe larger than the snowmobile, leading to impossible source localization. The corresponding Clean-SC map is shown in Fig. 4(b). With Clean-SC, the noise source map is clearly improved and two main spots are detected. One spot is close to the exhaust and the second corresponds to the track. Therefore at low frequency, beamforming cannot effectively discriminate the relatively compact noise sources of a snowmobile. In contrast, Clean-SC allows detection of low frequency broadband noise such as the exhaust or the snow-track noise.

## 5. Conclusion

Novel acoustic imaging results of snowmobile pass-by noise using a large microphone array have been presented. The experiments involved a 193-microphone Underbrink array and synchronization of acoustic with video data provided by a high-speed camera. The noise source maps provide useful insights into the various noise sources (engine, exhaust, and track) as well as quantitative information on the insertion loss provided by the engine hood. In low frequency, conventional beamforming cannot

effectively discriminate the various noise sources. In contrast, the deconvolution technique Clean-SC provides much better source discrimination.

**Acknowledgments**

The authors wish to thank NSERC (Natural Sciences and Engineering Research council of Canada) for its financial and technical support.

**References and links**

[1]T. Leroux, M. Gendron, and P. Andree, "Enquete socio-acoustique sur le bruit cause par la circulation des motoneiges (Socio-acoustic noise survey due to snowmobile pass-by)," Institut National de Sante Publique du Quebec (INSPQ) (2010), pp. 1–207.

[2]J. Blough, G. Gwaltney, and J. Vizanko, "Quantifying how the environment effects sae-j192 pass-by noise testing of snowmobiles," SAE Technical Paper 01-2414, pp. 1–11 (2005).

[3]C. Menge, J. Ross, and R. Ernenwein, "Noise data from snowmobile pass-bys: The significance of frequency content," Society of Automotive Engineers (SAE) 2002-01-2765 (2002), pp. 1–10.

[4]L. Liikonen, M. Alanko, S. Jokinen, I. Niskanen, and L. Virrankoski, "Snowmobile noise," Finnish Ministry of the Environment (2007), pp. 1–48.

[5]T. J. Mueller, *Aeroacoustic Measurements* (Springer, New York, 2002), 308 pp.

[6]Q. Wei, S. Zhong, and X. Huang, "Experimental evaluation of flow-induced noise in level flight of the pigeon (columba livia)," J. Acoust. Soc. Am. **134**(5), 57–63 (2013).

[7]B. Barsikow, W. F. King, and E. Peizenmaier, "Wheel/rail noise generated by a high-speed train investigated with a line array of microphone," J. Sound Vib. **118**, 99–122 (1987).

[8]C. Camier, J.-F. Blais, R. Lapointe, and A. Berry, "A time-domain analysis of 3d non-uniform moving acoustic sources: Application to source identification and absolute quantification via beamforming," in *4th Berlin Beamforming Conference*, Berlin, Germany (2012), pp. 1–17.

[9]D. Yang, Z. Wang, B. Li, and X. Lian, "Development and calibration of acoustic video camera system for moving vehicles," J. Sound Vib. **330**, 2457–2469 (2011).

[10]T. Padois, C. Prax, and V. Valeau, "Numerical validation of shear flow corrections for beamforming acoustic source localisation in open wind-tunnels," Appl. Acoust. **74**, 591–601 (2013).

[11]S. Krober, K. Ehrenfried, L. Koop, A. Lauterbach, and A. Henning, "Systematic comparison of microphone array measurements in open and closed wind tunnels," in *16th AIAA/CEAS Aeroacoustics Conference*, AIAA-2010-3734, Stockholm, Sweden (June 2010), pp. 1–15.

[12]C. Bahr, N. S. Zawodny, T. Yardibi, and F. Liu, "Shear layer correction validation using a non-intrusive acoustic point source," in *16th AIAA/CEAS Aeroacoustics Conference*, AIAA-2010-3735, Stockholm, Sweden (June 2010), pp. 1–20.

[13]P. Sijtsma, "Clean based on spatial source coherence," Int. J. Aeroacoust. **6**, 357–374 (2007).

[14]T. F. Brooks and W. M. Humphreys, "A deconvolution approach for the mapping of acoustic sources (damas) determined from phased microphone arrays," J. Sound Vib. **294**, 856–879 (2006).

[15]T. Padois, P.-A. Gauthier, and A. Berry, "Inverse problem with beamforming regularization matrix applied to sound source localization in closed wind-tunnel using microphone array," J. Sound Vib. **333**, 6858–6868 (2014).

[16]T. Padois and Alain Berry, "Orthogonal matching pursuit applied to the deconvolution approach for the mapping of acoustic sources inverse problem," J. Acoust. Soc. Am. **138**(6), 3678–3685 (2015).